Organic Dust, Lipopolysaccharide, and Peptidoglycan Inhalant Exposures Result in Bone Loss/Disease

Anand Dusad[1], Geoff M. Thiele[1,4], Lynell W. Klassen[1,4], Angela M. Gleason[2], Christopher Bauer[2], Ted R. Mikuls[1,4], Michael J. Duryee[1], William W. West[3], Debra J. Romberger[2,4], and Jill A. Poole[2]

[1]Division of Rheumatology, [2]Pulmonary, Critical Care, Sleep, and Allergy Division, Department of Internal Medicine, and [3]Department of Pathology and Microbiology, University of Nebraska Medical Center, Omaha, Nebraska; and [4]Veterans Administration Nebraska Western Iowa Healthcare System, Omaha, Nebraska

Skeletal health consequences associated with chronic inflammatory respiratory disease, and particularly chronic obstructive pulmonary disease (COPD), contribute to overall disease morbidity. Agricultural environmental exposures induce significant airway diseases, including COPD. However, animal models to understand inhalant exposure–induced lung injury and bone disease have not been described. Using micro–computed tomography (micro-CT) imaging technology and histology, bone quantity and quality measurements were investigated in mice after repetitive intranasal inhalation exposures to complex organic dust extracts (ODEs) from swine confinement facilities. Comparison experiments with LPS and peptidoglycan (PGN) alone were also performed. After 3 weeks of repetitive ODE inhalation exposure, significant loss of bone mineral density and trabecular bone volume fraction was evident, with altered morphological microarchitecture changes in the trabecular bone, compared with saline-treated control animals. Torsional resistance was also significantly reduced. Compared with saline treatment, ODE-treated mice demonstrated decreased collagen and proteoglycan content in their articular cartilage, according to histopathology. Significant bone deterioration was also evident after repetitive intranasal inhalant treatment with LPS and PGN. These findings were not secondary to animal distress, and not entirely dependent on the degree of induced lung parenchymal inflammation. Repetitive LPS treatment demonstrated the most pronounced changes in bone parameters, and PGN treatment resulted in the greatest lung parenchymal inflammatory changes. Collectively, repetitive inhalation exposures to noninfectious inflammatory agents such as complex organic dust, LPS, and PGN resulted in bone loss. This animal model may contribute to efforts toward understanding the mechanisms and evaluating the therapeutics associated with adverse skeletal health consequences after subchronic airway injury.

Keywords: lung; inflammation; bone; imaging; bioaerosol

The systemic consequences of chronic inflammatory airway diseases are increasingly recognized for their contributions to overall disease morbidity (1, 2). In patients with chronic obstructive pulmonary disease (COPD), an increased prevalence of osteoporosis and of low bone mineral density (BMD) is evident (2–4). Although risk factors such as low body mass index, sex, age, steroid use, cigarette smoking, and severity of obstruction have been associated with bone loss, low BMD in obstructive lung disease has also been demonstrated to occur independent of these established risk factors or severity of obstruction (3, 4). This observation implicates a pathogenic association between airway disease and bone mineralization. However, animal models and/or mechanisms to explain this relationship between inflammatory lung disease and bone loss are lacking, and would be important in the development of novel therapies to prevent or stop disease progression.

Previously, our group characterized the airway inflammatory response after repetitive exposures to animal-confinement (e.g., swine) organic dusts and their components in an animal model, for a better understanding of the mechanisms underlying inhalant-induced lung injury in exposed workers (5, 6). Agricultural environmental exposure has been recognized as an independent risk factor for asthma symptoms, chronic bronchitis, and COPD development in humans (7). Farming is also a known occupational hazard for developing musculoskeletal diseases such as osteoarthritis (OA) and rheumatoid arthritis (RA) (8–12). The organic dust exposure is complex, involving a wide diversity of microbial motifs (e.g., peptidoglycans [PGNs] and endotoxin) and particulate matter, which elicit airway inflammatory responses in mice (7, 13). Namely, repetitive organic dust exposures induce the development of lymphoid aggregates and peribronchiolar/vascular inflammation, comprised of T and B lymphocytes and macrophages with associated neutrophil recruitment (5, 14, 15). Although LPS remains an important component, the inflammatory lung response is not entirely dependent on LPS (6, 16), and moreover, Gram-positive components, including PGN (7, 13, 17), appear to be the major factors driving lung consequences. However, the systemic effects of bone disease after repetitive inhalant exposure to organic dust and its main components, LPS and PGN, have not been described.

Based on the collective evidence for the association of chronic airway inflammatory diseases with bone and musculoskeletal diseases, we hypothesized that bone-related systemic consequences would occur in an organic dust–induced airway disease animal model. To test this hypothesis, C57BL/6 mice were repetitively treated with organic dust extract (ODE) according to an established protocol for 3 weeks, whereupon the legs of the mice were excised and investigated for BMD and other structural bone parameters via micro–computed tomography (micro-CT) imaging and histology. Because our studies demonstrated a significant loss of bone density and volume along with the morphologic deterioration of bone tissue after repetitive ODE exposures, comparison experiments with intranasal inhalant exposures to LPS and PGN (important microbial products in the organic dust and other exposure environments) (18) were also undertaken. Repetitive inhalant exposures to LPS and PGN alone also resulted in significant bone loss. This study

(*Received in original form April 19, 2013 and in final form June 6, 2013*)

This study was supported by grants from the National Institute of Environmental Health Sciences of the National Institutes of Health (R01 ES019325 to J.A.P.), the Nebraska Arthritis Outcomes Research Center (T.R.M. and G.M.T.), the American College of Rheumatology/Rheumatology Research Foundation (T.R.M.), and the Department of Internal Medicine, University of Nebraska Medical Center (L.W.K.). This work was also supported by the Central States Center for Agricultural Safety and Health.

Correspondence and requests for reprints should be addressed to Jill A. Poole, M.D., Pulmonary, Critical Care, Sleep, and Allergy Division, Department of Internal Medicine, University of Nebraska Medical Center, 985300 The Nebraska Medical Center, Omaha, NE 68198-5300. E-mail: japoole@unmc.edu

This article has an online supplement, which is accessible from this issue's table of contents at www.atsjournals.org

Am J Respir Cell Mol Biol Vol 49, Iss. 5, pp 829–836, Nov 2013
Published 2013 by the American Thoracic Society
Originally Published in Press as DOI: 10.1165/rcmb.2013-0178OC on June 19, 2013
Internet address: www.atsjournals.org

strongly suggests that this animal model may be important for future studies investigating the mechanisms and preventative and/or treatment options of generalized bone loss and disease after repetitive inflammatory inhalant exposures.

MATERIALS AND METHODS

Bioaerosol Agents

Aqueous ODE was collected and prepared as previously described (14), and as described in the online supplement. To broaden the applicability of systemic ODE-induced lung injury bone consequences, comparison experiments were performed with LPS (100 ng per 30 μl, which is approximately double the concentration of detectable LPS in 12.5% ODE, from *Escherichia coli* O55:B5; Sigma Chemical Co., St. Louis, MO) and *Staphylococcus aureus* PGN (100 μg per 30 μl; Sigma Chemical Co.), which also remains consistent with our previous work comparing ODE-induced responses to PGN (6).

Animal Model

Male C57BL/6 mice (6–8 wk old, purchased from the Jackson Laboratory, Bar Harbor, ME) received an intranasal inhalation of sterile saline (PBS), 12.5% ODE, LPS (100 ng), and PGN (100 μg), according to an established protocol (6) daily for 3 weeks, with weekends excluded. No mice exhibited respiratory distress throughout the treatment period. All animal procedures were approved by the Institutional Animal Care and Use Committee at the University of Nebraska Medical Center, according to National Institutes of Health guidelines for the use of rodents.

Micro-CT Analysis

After repetitive inhalational exposures, the mice were killed 24 hours after the final exposure. Hind limbs were isolated/dissected above the ankle and fixed in 10% buffered formalin for 48 hours. Owing to its high-resolution imaging and nondestructive approach, micro-CT is considered the gold standard for analyzing and quantifying three-dimensional (3D) changes in bone morphology (19). Scanning details and analysis details using the micro-CT system (SkyScan 1172; SkyScan, Aartselaar, Belgium) are described in the online supplement.

Histopathology

Bones. After micro-CT imaging, formalin-fixed hind limbs were decalcified in Immunocal (American MasterTech Scientific, Lodi, CA) (20). Hind limbs were processed, sectioned (4–5 μm), and stained with hematoxylin and eosin. Articular cartilage morphology and proteoglycan content were studied using safranin O/fast green (SOFG) staining. Because imaging modalities fail to quantify changes in the organic component of extracellular bone matrix, of which more than 90% is collagen (21), we used previously described modified Masson staining to investigate collagen deposition. Slides were scanned with an iScan Coreo Au slide scanner (Ventana, Tucson, AZ) by the Tissue Sciences Facility at the Department of Pathology and Microbiology (University of Nebraska Medical Center, Omaha, NE), and converted into digital format for further analysis and quantification.

Lungs. Whole lungs were excised and inflated to 20 cm H_2O pressure with 10% formalin (Sigma Chemical Co.) to preserve the pulmonary architecture. Entire lung sections (4–5 μm) were semiquantitatively assessed for their degree of inflammation and for the distribution of inflammation by a pathologist blinded to the treatment conditions and using a previously described scoring system (5, 6). For each inflammatory parameter, an independently assigned value from 0–3 was given, with higher scores indicating greater inflammatory changes in the lung.

Statistical Methods

Data are presented as means ± SDs or as SEMs, as indicated. Statistical analyses were performed using the Student *t* test or two-tailed Mann-Whitney test, with one-way ANOVA and the Tukey *post hoc* test as appropriate. All statistical analyses were performed using SPSS software (SPSS, Inc., Chicago, IL), and significance was set at $P < 0.05$.

RESULTS

Inhalant Exposures Were Well-Tolerated

During all experimental studies, a gradual increase was evident in the body weight of all animals in all treatment groups. Specifically, mice treated with saline gained an average of 1.4 g (SD, 0.55 g), ODE-treated mice gained an average of 1.6 g (SD, 0.77 g), LPS-treated mice gained an average of 0.8 g (SD, 0.51 g), and PGN-treated mice gained an average of 2.3 g (SD, 0.63 g). Although animals in the LPS treatment group gained less weight compared with the other treatment groups, these differences were not statistically significant ($P > 0.05$). Animals in all groups showed normal activity levels, with no signs of sickness, distress, or restricted mobility.

Intranasal Inhalation of Organic Dust Causes Significant Bone Loss

After 3 weeks of repetitive intranasal inhalational exposure to ODE, changes in the BMD, volume, and morphology of the trabecular bone were evaluated in the distal calcaneus using micro-CT in comparison with saline-treated animals (Figures 1 and 2). Our two-dimensional (2D)-reconstructed (Figure 1A) and 3D-reconstructed (Figure 1B) CT images indicated clear evidence of trabecular as well as cortical bone loss. Parameters describing both bone quantity and quality between groups were determined as described in the online supplement. Compared with the saline treatment group, mice treated with ODE showed a significant loss of BMD (Figure 2A; $P = 0.002$, $n = 4$ mice/group). This loss of mineralization was also accompanied by a significant decrease in the total trabecular bone volume fraction (BV/TV; $P = 0.003$) in the ODE treatment group, s compared with saline-treated animals (Figure 2B). In addition, ODE-treated animals also demonstrated a significant increase in their specific bone surface (BS/BV; $P = 0.004$), indicating increased bone resorption (Figure 2C).

ODE treatment also resulted in altered morphological changes in the microarchitecture and structure of the trabecular bone (Figures 2C–2H). A significant decrease in trabecular thickness (Tb Th, mm; $P = 0.010$) and trabecular number (Tb N, mm^{-1}; $P = 0.006$), and an increase in trabecular separation (Tb Sp, mm; $P = 0.028$), was found in the ODE-treated animals, compared with the saline control mice, which indicates substantial deterioration of the trabecular microarchitecture. A significant increase of rod-like trabecular structures was also evident, as shown by an increased structural model index (SMI, +420%; $P = 0.002$) after ODE treatment when compared with the saline control animals. The SMI represents the transition of a normal plate-like structure (SMI = 0) into a rod-like trabecular structure (SMI = 3) (22). Repetitive ODE treatment also resulted in a significantly disconnected trabecular bone structure, as shown by the trabecular pattern factor (Tb Pf, +325%; $P = 0.003$). Collectively, an increase in both SMI and Tb Pf suggests that the inhalational lung injury caused by ODE exposure induced significant bone loss in the trabecular structure (23–25).

Bone mechanical properties can be estimated by the polar moment of inertia (MMI, mm^4), a measure of torsional resistance (26), which is an indicator of the deterioration of bone quantity and quality. Indeed, repetitive ODE treatment resulted in a significant loss of mechanical properties, as estimated by the MMI (−43%; $P = 0.003$), compared with saline treatment (Figure 2I).

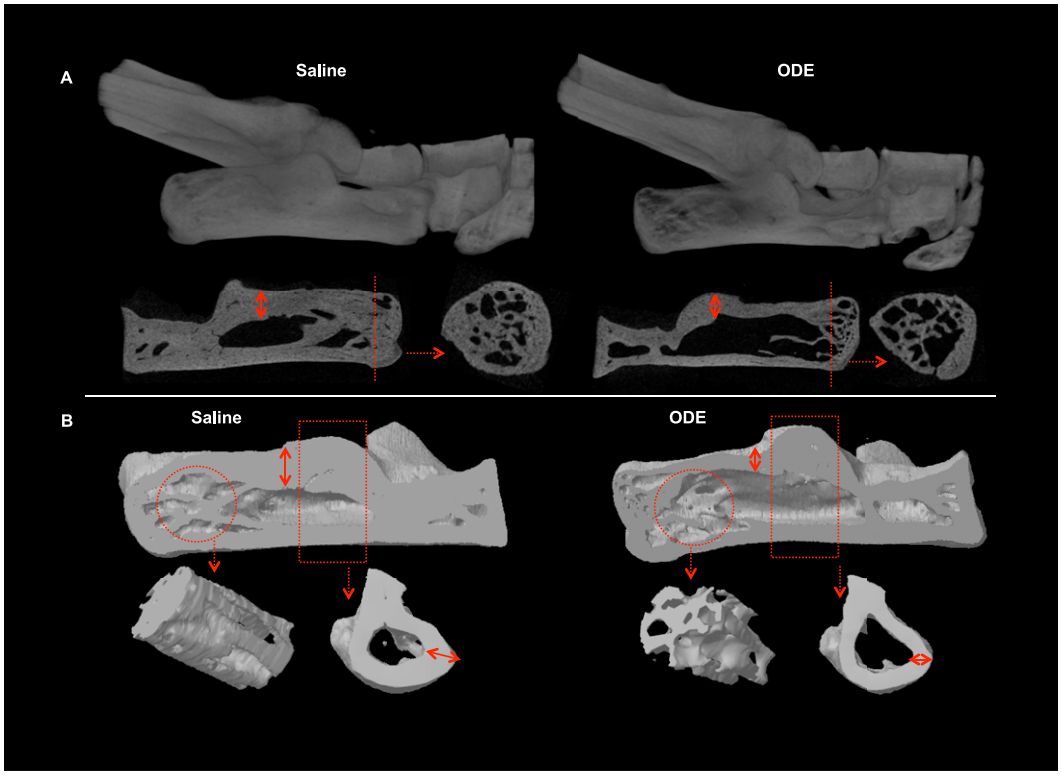

Figure 1. Bone loss after repetitive treatment with organic dust. (*A*) Representative two-dimensional (2D) images (1 of 4 animals per group, *top*) of ankles in animals repetitively treated for 3 weeks with intranasal saline (control) and organic dust extract (ODE), with coronal and transaxial images of the calcaneus (*bottom*). *Dotted red line* on the coronal view represents the transaxial cut. *Dotted red arrows* indicate the cross-section. Note the substantial loss of trabecular bone in the distal calcaneus of the ODE-treated group. (*B*) Three-dimensional (3D) reconstructed images from the saline-treated and ODE-treated groups (*top*). Reconstructive images are shown of region of interest (*circle*) in the distal calcaneus, where micro–computed tomography (micro-CT) analysis was performed, along with the proximal cortical bone (*rectangle, bottom*). Note the substantial loss of cortical bone represented as cortical thinning (*double arrow*) in both 2D and 3D images.

Bone Histology

To corroborate the CT findings, bone histomorphometric changes were investigated, and the results confirmed our micro-CT findings. Trabecular bone volume was decreased in the distal calcaneus and cuboidal bones after ODE treatment, compared with saline treatment (Figure 3). A higher degree of cellular infiltrate in the marrow cavity of the ODE treatment group was also observed, in comparison with the saline control animals. The articular cartilage of the calcaneo-cuboidal joint was examined using the SOFG stain, which demonstrated a lack of uniformity and a loss of proteoglycan content in ODE-treated mice compared with saline-treated mice (Figure 3). Using modified Masson staining for collagen experiments, mice treated with ODE demonstrated depleted collagen content of the calcaneus (Figure 3), suggesting a loss of organic bone matrix. Consistent with the micro-CT findings, a decreased cortical thickness of the calcaneus was also evident in all stained bone sections (Figure 3).

Repetitive Inhalation Treatment with LPS and PGN Results in Bone Loss

Because ODE intranasal inhalation treatment resulted in significant bone loss, we investigated the effects of intranasal inhalations of LPS and PGN alone in side-by-side experiments with ODE (and saline control) to further delineate important inhalation agents potentially mediating the observed bone response with ODE. Confirming earlier findings (Figures 1 and 2), micro-CT analysis showed significant bone deterioration after ODE treatment group (Table 1 and data not shown), but we also found significant bone loss after LPS and PGN treatment, compared with saline treatment (Table 1 and Figure 4). These differences between groups were quantitated, as shown in Table 1. To summarize, significant loss in bone density and volume was observed in the ODE-treated, LPS-treated, and PGN-treated groups, compared with the saline group. Mean specific bone surface was increased after ODE ($P = 0.053$), LPS ($P = 0.006$), and PGN ($P = 0.327$) treatments when compared with saline treatment. The mean trabecular thickness was decreased in the ODE, LPS, and PGN groups, compared with the saline group. Trabecular numbers were significantly reduced in the ODE, LPS, and PGN treatment groups compared with the saline group, with no significant differences between exposed groups. Trabecular structural changes, as indicated by SMI and Tb Pf, were found to be significantly increased in the ODE, LPS, and PGN treatment groups, compared with the saline group. Torsional resistance was also significantly decreased after ODE, LPS, and PGN treatment, compared with the saline group. Interestingly, LPS treatment demonstrated the most pronounced bone deterioration, and statistically significant differences were found in BMD, BV/TV, BS/BV, Tb Th, and MMI in comparison with PGN treatment (Table 1).

Lung Inflammation after Repetitive Treatment with ODE, LPS, and PGN

Previously, we established that repetitive intranasal inhalations of ODE and PGN result in lung histopathologic changes, marked by the development of lymphoid aggregates and increased alveolar and bronchiolar compartment inflammation (5). In the present study, lungs from the same mice used in the bone experiments depicted in Figure 4 and Table 1 were processed and hematoxylin and eosin–stained (Figures 5A–5D), and semiquantitatively assessed for inflammatory changes (Figure 5E). Consistent with our previous work (5, 6), repetitive ODE and PGN treatment resulted in significant increases in all inflammatory parameters, including lymphoid aggregates and alveolar and bronchiolar

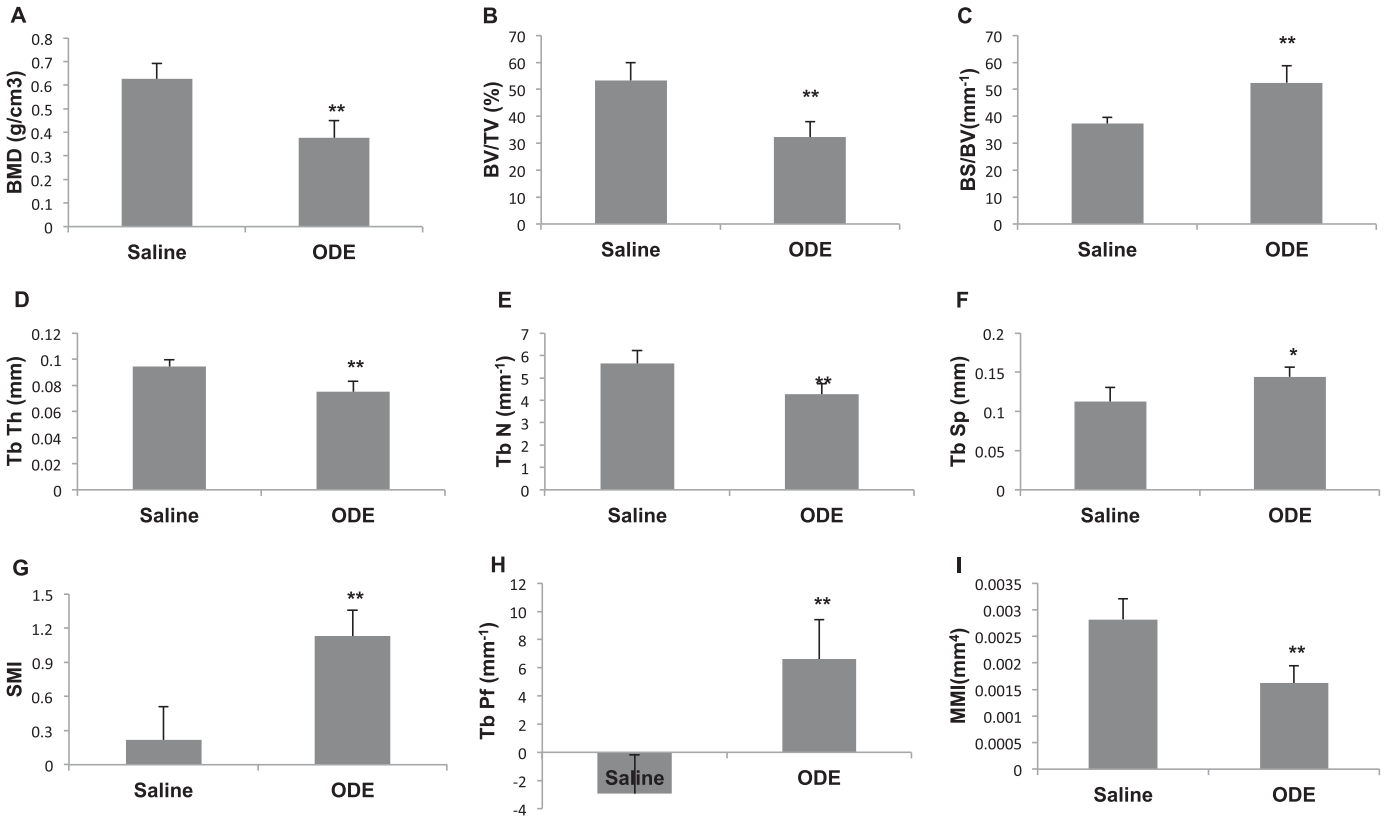

Figure 2. Repetitive ODE inhalation exposure results in decreased bone quality and quantity according to micro-CT imaging analysis. After 3 weeks of repetitive intranasal inhalation treatment with saline (control) and ODE, the animals were killed, and their calcaneus bones were subjected to micro-CT analysis. ODE induced significant changes in mean parameters of bone quality and bone quantity, as measured in the trabecular bone of the distal calcaneus of these animals ($n = 4$/group). Specifically, differences in (*A*) bone mineral density (BMD), (*B*) bone volume to tissue volume ratio (BV/TV), (*C*) bone surface to bone volume ratio (BS/BV), (*D*) trabecular thickness (Tb Th), (*E*) trabecular number (Tb N), (*F*) trabecular separation (Tb Sp), (*G*) structural model index (SMI), (*H*) trabecular pattern factor (Tb Pf), and (*I*) the polar moment of inertia (MMI) are shown. *Error bars* represent SDs. *$P < 0.05$ and **$P < 0.01$ indicate statistical significance (Student *t* test) between saline-treated and ODE-treated mice.

compartment inflammation, compared with saline-treated animals. However, repetitive LPS treatment resulted in subtle, but nonsignificant, increases in alveolar and bronchiolar compartment inflammation. Overall, PGN treatment resulted in the most pronounced lung parenchymal inflammatory changes, and statistically significant differences were found in all inflammatory parameters in comparison with LPS treatment (Figure 5E).

DISCUSSION

This study demonstrated significant bone loss and disease after repetitive inhalation exposure to complex ODE, LPS, and PGN in mice. This was not secondary to animal distress or weight loss, and was not entirely dependent on the degree of induced lung parenchymal inflammation. Bone deterioration was marked by adverse effects on the parameters of both bone quantity and quality, which culminated in the loss of bone strength and mechanical properties. The findings demonstrated by micro-CT were confirmed by bone histology, which also demonstrated decreased bone collagen and depleted proteoglycan within the articular cartilage. Collectively, and to the best of our knowledge, this is the first *in vivo* animal report to demonstrate that repetitive inhalation exposure to inflammatory agents such as organic dust, LPS, and PGN causes bone loss. This animal model may substantially contribute to understanding the mechanisms underlying systemic manifestations of chronic, noninfectious lung disease.

The substantial loss of bone quantity and the deterioration of bone quality described are suggestive of osteoporosis (27, 28), a known risk factor for fractures. Osteoporosis is defined not only by low bone mass, but also by microarchitectural deterioration of the bone tissue, which apart from BMD plays an important role in defining the biomechanical properties of skeletal tissue (27, 29). In addition, the degradation of organic extracellular bone matrix affects fracture fragility in osteoporosis (30). With the emergence of newer imaging technologies (e.g., micro-CT imaging), numerous studies have validated the importance of assessing both bone quantity and quality to achieve an overall view of skeletal health (27–29, 31, 32). Using this new and validated approach, our experiments revealed a significant depletion of bone mass and disconnected trabecular structure with a predominance of rod-like trabeculae and a loss of mechanical strength after repetitive inhalant exposure to ODE, LPS, and PGN.

Bone tissue maintains a homeostatic environment owing to the synergy between osteoblasts (bone-forming) and osteoclasts (bone-resorbing). Osteoclasts are multinucleated giant cells, differentiated from the monocytic/macrophage lineage of hematopoietic precursor cells (33). In certain rheumatologic diseases such as rheumatoid arthritis, localized and systemic inflammation causes an imbalance of this equilibrium, currently thought to be secondary to increased osteoclast activity (34). In addition, bacterial cell-wall components, including but not limited to LPS and PGN, have been implicated in directly mediating inflammatory skeletal diseases, including periodontitis, arthritis, and

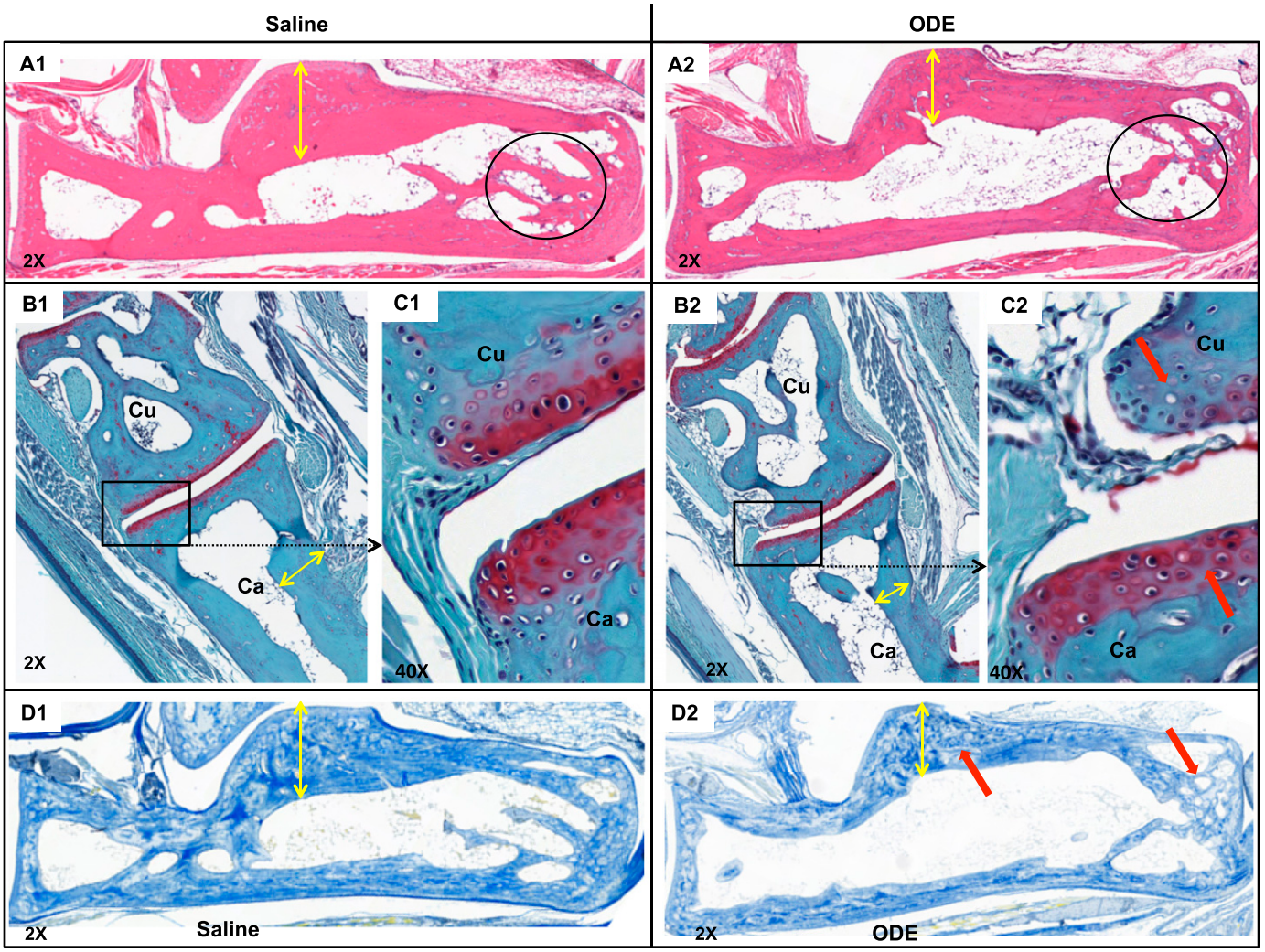

Figure 3. Repetitive treatment with ODE results in bone loss parameters according to histopathology. After micro-CT imaging, right hind limbs from mice exposed to saline (control) and ODE for 3 weeks were decalcified, sectioned, and stained. Sections of one mouse per treatment group were stained with hematoxylin and eosin (*A*), safranin O/fast green (SOFG) (*B*), or modified Masson (*D*), and are shown at ×2 magnification. (*A*) In accordance with micro-CT data and images, note the decreased trabecular bone in the distal calcaneus (*circle*) after hematoxylin and eosin staining. (*B* and *C*) Representative images of the calcaneo (Ca)–cuboidal (Cu) joint after SOFG staining at ×2 (*B*) and ×40 (*C*) demonstrate changes in articular cartilage. Note the depletion of proteoglycan and loss of uniformity in the articular cartilage of the ODE treatment group (*C2*, *bold red arrows*). (*D*) Modified Masson staining indicates loss of collagen in the ODE-exposed group (*D2*, *bold red arrows*). All images of the ODE treatment group show a decreased cortical thickness of the calcaneus (*A2*, *B2*, and *D2*, *double arrows* indicate cortical thickness).

osteomyelitis (35, 36). During osteoclast differentiation, modulating the gene expression of Toll-like receptors (TLRs) results in the predominant expression of TLR2 and TLR4 (33). Although both macrophage-colony stimulating factor (M-CSF) and the receptor activator of the NF-κB ligand are essential for osteoclastogenesis, studies have shown that LPS and PGN affect osteoclastogenesis in a dose-dependent manner (36, 37). Moreover, LPS through TLR4 recognition and PGN through TLR2 recognition initiate an inflammatory cascade (i.e., IL-1β, IL-6, and TNF-α release) via the activation of NF-κB and mitogen-activated protein kinase, resulting in bone resorption (33, 36, 37). In our findings of inhalational lung injury–induced bone loss, the possibility exists that these bacterial components escaped into the systemic circulation to affect skeletal health directly. However, lung-produced inflammatory mediators may also have escaped into the systemic circulation, where they directly or indirectly activated osteoclasts or disrupted the osteoclast–osteoblast equilibrium. Indeed, others have shown that inflamed COPD lungs release a variety of inflammatory mediators (e.g., IL-6 and granulocyte/macrophage colony–stimulating factor) that promote the recruitment of inflammatory cells into plaques affecting plaque stability, resulting in cardiovascular disease (38–40). Future studies to explore these various mechanisms underlying inhalational lung injury–induced bone disease are warranted.

A divergence was evident between lung parenchymal inflammation and degree of bone loss. Namely, the LPS exposure group showed mild and nonsignificant changes in lung histopathology (Figures 5C and 5E), and yet bone deterioration was greatest in mice repetitively exposed to LPS (Table 1). In contrast, repetitive PGN treatments resulted in the greatest changes in lung histopathology (Figures 5D and 5E), but the lowest amount of comparable bone changes (Table 1). Although part of this response may be attributable to the concentrations used, it is more likely explained by the differing host effects induced by these bacterial products. As previously reported (13) and

TABLE 1. QUANTITATIVE OVERVIEW OF BONE LOSS ACCORDING TO MICRO-CT IMAGING

Parameter	Saline ($n = 3$)	ODE ($n = 4$)	LPS ($n = 4$)	PGN ($n = 4$)	ANOVA (P Value)
Bone mineral density (g/mm^3)	0.63 ± 0.03	0.48 ± 0.04*	0.43 ± 0.02*,†	0.53 ± 0.06*	0.000
Percent bone volume	51.38 ± 2.54	38.40 ± 2.80*	34.65 ± 1.86*,†	43.50 ± 5.46*	0.000
Specific bone surface (mm^{-1})	39.95 ± 4.13	48.07 ± 4.21	52.76 ± 1.26*,†	43.79 ± 7.57	0.027
Trabecular pattern factor (mm^{-1})	−0.83 ± 1.93	4.75 ± 0.20*	4.75 ± 1.92*	2.81 ± 2.57*	0.008
Structural model index	0.53 ± 0.27	1.09 ± 0.07*	0.95 ± 0.15*	0.96 ± 0.22*	0.012
Trabecular thickness (mm)	0.091 ± 0.007	0.080 ± 0.008	0.073 ± 0.002*,†	0.087 ± 0.011	0.042
Trabecular number (mm^{-1})	5.64 ± 0.16	4.76 ± 0.19*	4.73 ± 0.26*	5.01 ± 0.40*	0.005
Trabecular separation (mm)	0.11 ± 0.007	0.13 ± 0.005	0.12 ± 0.004	0.12 ± 0.014	0.094
Polar moment of inertia (mm^4)	0.0030 ± 0.00010	0.0020 ± 0.00017*	0.0017 ± 0.00008*,†,‡	0.0022 ± 0.00027*	0.000

Definition of abbreviations: micro-CT, micro–computed tomography; ODE, organic dust extract; PGN, peptidoglycan.
*$P < 0.05$, †$P < 0.05$, and ‡$P < 0.05$ represent statistical significance versus saline, PGN, and ODE, respectively, using least significance difference (LSD) as *post hoc* test for multiple comparisons within the groups. Data are represented as means ± SDs.

described in the online supplement, the ODE used is a complex biological agent comprised of particulate matter and significant quantities of LPS and PGN (i.e., microbial components of Gram-negative and Gram-positive bacteria, respectively). The LPS dose chosen was double the amount detected in ODE, to prevent an underestimation of its role. In addition, it was previously shown that LPS may not be a major driver of swine confinement organic dust–induced lung inflammation. Specifically, TLR4-deficient mice were only minimally protected from acute swine barn air–induced inflammation (16), and dust scrubbed of LPS retains significant inflammatory potential (7, 13). Accumulating evidence suggests that PGN is a major driver of animal confinement organic dust–induced lung inflammation, because TLR2-deficient mice are significantly (but not completely) protected from acute and repetitive organic dust–induced airway inflammation (6). Gram-positive bacteria are also abundant in these agricultural environments (13, 17), and moreover, TLR2 gene polymorphisms, but not TLR4 gene polymorphisms, were recently associated with lung function in workers at swine operations (41). Thus, these current studies parallel previous work demonstrating an important role for PGN in mediating dust-induced lung inflammatory consequences. However (and importantly), these studies suggest that LPS may be the critical component in mediating the systemic bone loss consequences.

The lack of a comparable effect on bone health by PGN may be explained by its multilayered and cross-linked rigid structure (42). Owing to these unique structural characteristics, the inhalation of PGN may affect the processing and clearance of this molecule in the respiratory system. Indeed, others have shown that PGN from *S. aureus* failed to induce arthritis when digested and fragmented (43), suggesting that only a part of these long-chained structures has proinflammatory properties (44). Future studies are warranted to dissect these potential mechanisms. Future lines of epidemiologic research may also be needed to determine links between occupational exposures and bone loss or fractures. Furthermore, a clinical implication of this study involves the need to promote the use of protective respiratory gear for workers in agricultural and/or organic dust environments, to protect not only their lungs, but also, potentially, their bones.

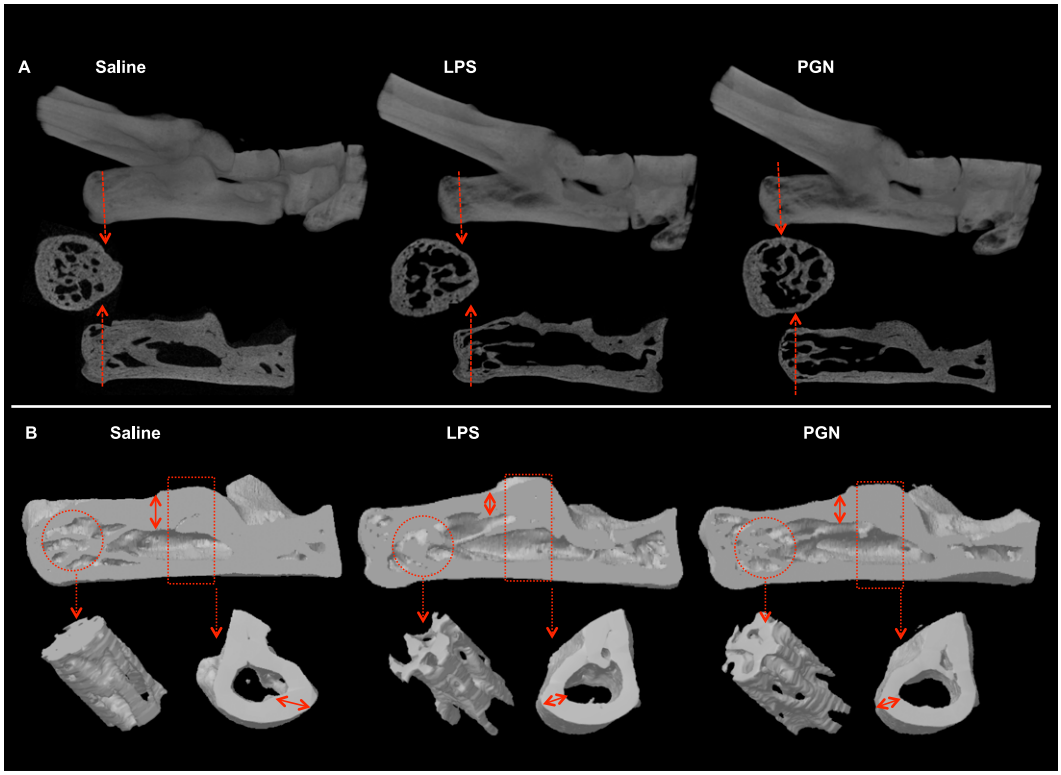

Figure 4. Repetitive inhalation exposure to LPS and peptidoglycan (PGN) results in bone loss according to micro-CT imaging analysis. (*A*) Representative 2D images of ankle (*top*) in animals (1 of 4 animals per group) repetitively treated for 3 weeks with LPS, PGN, or saline by intranasal inhalation method, with coronal and transaxial images of the calcaneus (*bottom*). *Dotted red line* on the coronal view represents the transaxial cut. *Dotted red arrows* indicate cross section. (*B*) 3D reconstructed images of one of four mice per treatment group, i.e., saline, LPS, and PGN (*top*). Reconstructive images of region of interest (*circle*) are shown in the distal calcaneus, where micro-CT analysis was performed, along with the proximal cortical bone (*rectangle*, *bottom*). Note the substantial loss of cortical bone, represented as cortical thinning (*double arrow*) in both 2D and 3D images.

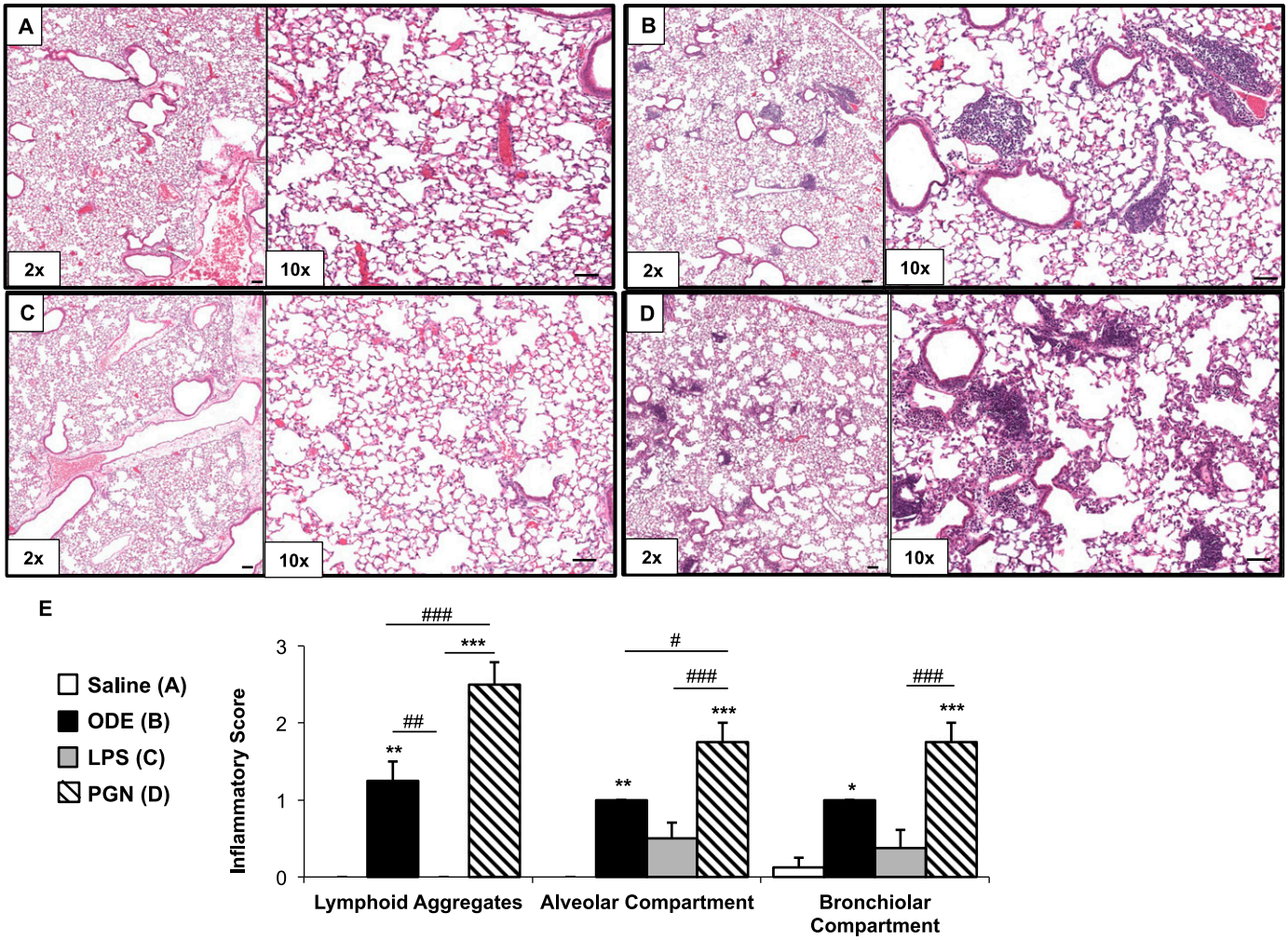

Figure 5. (*A–E*) Lung inflammation after repetitive treatment with ODE, LPS, and PGN. Mice were intranasally treated with saline control (*A*), ODE (*B*, 12.5%), LPS (*C*, 100 ng), and PGN (*D*, 100 μg) daily for 3 weeks. A representative 4–5-μm-thick section (hematoxylin and eosin–stained) of one of four mice per treatment group is shown at ×10 magnification (*A–D*). (*E*) Mean semiquantitative distribution of inflammatory score of lung lymphoid aggregates, alveolar inflammation, and bronchiolar inflammation in mice ($n = 4$ mice per group). *Error bars* represent SEs. Statistically significant differences are denoted by *asterisks* (*$P < 0.05$, **$P < 0.01$, and ***$P < 0.001$), compared with saline treatment. $^{\#}P < 0.05$, $^{\#\#}P < 0.01$, and $^{\#\#\#}P < 0.001$ denote significant differences between groups, as indicated. One-way ANOVA was performed, with Tukey *post hoc* test comparison. *Line scale* represents 60 μm.

In conclusion, organic dust from swine confinement facilities promoted systemic bone loss, with LPS playing a more substantial role than PGN in terms of degrading skeletal health. However, in the same animals, ODE and PGN showed considerable lung pathology, with PGN alone demonstrating the most robust lung inflammatory response. Overall, this information suggests that the inhalation of varying microbial motifs may affect lung (localized) versus systemic consequences differently. With the use of micro-CT imaging technologies, we anticipate that this animal model demonstrating the intranasal inhalation of complex organic dust–induced, LPS-induced, and PGN-induced bone loss could not only be used to facilitate future mechanistic and interventional therapeutic studies, but could also be expanded to include other environmental exposure agents that might affect skeletal health.

Author disclosures are available with the text of this article at www.atsjournals.org.

Acknowledgments: The authors thank David Wert (Facility Supervisor, Tissue Science Facility, Department of Pathology and Microbiology, University of Nebraska Medical Center, Omaha, NE) for assistance with lung-tissue processing, sectioning, hematoxylin and eosin staining, and assistance with the digital microscopy images prepared for the manuscript.

References

1. Lehouck A, Boonen S, Decramer M, Janssens W. COPD, bone metabolism, and osteoporosis. *Chest* 2011;139:648–657.
2. Han MK, Agusti A, Calverley PM, Celli BR, Criner G, Curtis JL, Fabbri LM, Goldin JG, Jones PW, Macnee W, *et al.* Chronic obstructive pulmonary disease phenotypes: the future of COPD. *Am J Respir Crit Care Med* 2010;182:598–604.
3. Graat-Verboom L, Smeenk FW, van den Borne BE, Spruit MA, Jansen FH, van Enschot JW, Wouters EF. Progression of osteoporosis in patients with COPD: a 3-year follow up study. *Respir Med* 2012; 106:861–870.
4. Graat-Verboom L, Smeenk FW, van den Borne BE, Spruit MA, Donkers-van Rossum AB, Aarts RP, Wouters EF. Risk factors for osteoporosis in Caucasian patients with moderate chronic obstructive pulmonary disease: a case control study. *Bone* 2012;50:1234–1239.
5. Poole JA, Wyatt TA, Oldenburg PJ, Elliott MK, West WW, Sisson JH, Von Essen SG, Romberger DJ. Intranasal organic dust exposure–induced airway adaptation response marked by persistent lung inflammation and pathology in mice. *Am J Physiol Lung Cell Mol Physiol* 2009;296:L1085–L1095.
6. Poole JA, Wyatt TA, Kielian T, Oldenburg P, Gleason AM, Bauer A, Golden G, West WW, Sisson JH, Romberger DJ. Toll-like receptor 2

regulates organic dust–induced airway inflammation. *Am J Respir Cell Mol Biol* 2011;45:711–719.
7. Poole JA, Romberger DJ. Immunological and inflammatory responses to organic dust in agriculture. *Curr Opin Allergy Clin Immunol* 2012;12:126–132.
8. Walker-Bone K, Palmer KT. Musculoskeletal disorders in farmers and farm workers. *Occup Med* 2002;52:441–450.
9. Li X, Sundquist J, Sundquist K. Socioeconomic and occupational risk factors for rheumatoid arthritis: a nationwide study based on hospitalizations in Sweden. *J Rheumatol* 2008;35:986–991.
10. Kirkhorn S, Greenlee RT, Reeser JC. The epidemiology of agriculture-related osteoarthritis and its impact on occupational disability. *WMJ* 2003;102:38–44.
11. Thelin A, Vingard E, Holmberg S. Osteoarthritis of the hip joint and farm work. *Am J Ind Med* 2004;45:202–209.
12. Osborne A, Blake C, Fullen BM, Meredith D, Phelan J, McNamara J, Cunningham C. Risk factors for musculoskeletal disorders among farm owners and farm workers: a systematic review. *Am J Ind Med* 2012;55:376–389.
13. Poole JA, Dooley GP, Saito R, Burrell AM, Bailey KL, Romberger DJ, Mehaffy J, Reynolds SJ. Muramic acid, endotoxin, 3-hydroxy fatty acids, and ergosterol content explain monocyte and epithelial cell inflammatory responses to agricultural dusts. *J Toxicol Environ Health A* 2010;73:684–700.
14. Poole JA, Gleason AM, Bauer C, West WW, Alexis N, van Rooijen N, Reynolds SJ, Romberger DJ, Kielian TL. $CD11c^{+}$/$CD11b^{+}$ cells are critical for organic dust–elicited murine lung inflammation. *Am J Respir Cell Mol Biol* 2012;47:652–659.
15. Poole JA, Gleason AM, Bauer C, West WW, Alexis N, Reynolds SJ, Romberger DJ, Kielian TL. Alphabeta T cells and a mixed Th1/Th17 response are important in organic dust–induced airway disease. *Ann Allergy Asthma Immunol* 2012;109:266–273.
16. Charavaryamath C, Juneau V, Suri SS, Janardhan KS, Townsend H, Singh B. Role of Toll-like receptor 4 in lung inflammation following exposure to swine barn air. *Exp Lung Res* 2008;34:19–35.
17. Nehme B, Letourneau V, Forster RJ, Veillette M, Duchaine C. Culture-independent approach of the bacterial bioaerosol diversity in the standard swine confinement buildings, and assessment of the seasonal effect. *Environ Microbiol* 2008;10:665–675.
18. Poole JA. Farming-associated environmental exposures and effect on atopic diseases. *Ann Allergy Asthma Immunol* 2012;109:93–98.
19. Xie L, Lin AS, Levenston ME, Guldberg RE. Quantitative assessment of articular cartilage morphology via EPIC-microCT. *Osteoarthritis Cartilage* 2009;17:313–320.
20. Schopf L, Savinainen A, Anderson K, Kujawa J, DuPont M, Silva M, Siebert E, Chandra S, Morgan J, Gangurde P, *et al.* IKKbeta inhibition protects against bone and cartilage destruction in a rat model of rheumatoid arthritis. *Arthritis Rheum* 2006;54:3163–3173.
21. Paschalis EP, Shane E, Lyritis G, Skarantavos G, Mendelsohn R, Boskey AL. Bone fragility and collagen cross-links. *J Bone Miner Res* 2004;19:2000–2004.
22. Hildebrand T, Ruegsegger P. Quantification of bone microarchitecture with the structure model index. *Comput Methods Biomech Biomed Engin* 1997;1:15–23.
23. Vermeirsch H, Biermans R, Salmon PL, Meert TF. Evaluation of pain behavior and bone destruction in two arthritic models in guinea pig and rat. *Pharmacol Biochem Behav* 2007;87:349–359.
24. Nishida S, Tsurukami H, Sakai A, Sakata T, Ikeda S, Tanaka M, Ito M, Nakamura T. Stage-dependent changes in trabecular bone turnover and osteogenic capacity of marrow cells during development of Type II collagen–induced arthritis in mice. *Bone* 2002;30:872–879.
25. Yamane I, Hagino H, Okano T, Enokida M, Yamasaki D, Teshima R. Effect of minodronic acid (ONO-5920) on bone mineral density and arthritis in adult rats with collagen-induced arthritis. *Arthritis Rheum* 2003;48:1732–1741.
26. Bellido M, Lugo L, Roman-Blas JA, Castaneda S, Caeiro JR, Dapia S, Calvo E, Largo R, Herrero-Beaumont G. Subchondral bone microstructural damage by increased remodelling aggravates experimental osteoarthritis preceded by osteoporosis. *Arthritis Res Ther* 2010;12:R152.
27. Borah B, Gross GJ, Dufresne TE, Smith TS, Cockman MD, Chmielewski PA, Lundy MW, Hartke JR, Sod EW. Three-dimensional microimaging (MRmicroI and microCT), finite element modeling, and rapid prototyping provide unique insights into bone architecture in osteoporosis. *Anat Rec* 2001;265:101–110.
28. Ulrich D, van Rietbergen B, Laib A, Ruegsegger P. The ability of three-dimensional structural indices to reflect mechanical aspects of trabecular bone. *Bone* 1999;25:55–60.
29. Lespessailles E, Jullien A, Eynard E, Harba R, Jacquet G, Ildefonse JP, Ohley W, Benhamou CL. Biomechanical properties of human os calcanei: relationships with bone density and fractal evaluation of bone microarchitecture. *J Biomech* 1998;31:817–824.
30. Sroga GE, Vashishth D. Effects of bone matrix proteins on fracture and fragility in osteoporosis. *Curr Osteoporos Rep* 2012;10:141–150.
31. Topolinski T, Mazurkiewicz A, Jung S, Cichanski A, Nowicki K. Microarchitecture parameters describe bone structure and its strength better than BMD. *Sci World J* 2012;ID#502781:1–7.
32. Majumdar S, Genant HK, Grampp S, Newitt DC, Truong VH, Lin JC, Mathur A. Correlation of trabecular bone structure with age, bone mineral density, and osteoporotic status: *in vivo* studies in the distal radius using high resolution magnetic resonance imaging. *J Bone Miner Res* 1997;12:111–118.
33. Takami M, Kim N, Rho J, Choi Y. Stimulation by Toll-like receptors inhibits osteoclast differentiation. *J Immunol* 2002;169:1516–1523.
34. Walsh NC, Crotti TN, Goldring SR, Gravallese EM. Rheumatic diseases: the effects of inflammation on bone. *Immunol Rev* 2005;208:228–251.
35. Nair SP, Meghji S, Wilson M, Reddi K, White P, Henderson B. Bacterially induced bone destruction: mechanisms and misconceptions. *Infect Immun* 1996;64:2371–2380.
36. Kishimoto T, Kaneko T, Ukai T, Yokoyama M, Ayon Haro R, Yoshinaga Y, Yoshimura A, Hara Y. Peptidoglycan and lipopolysaccharide synergistically enhance bone resorption and osteoclastogenesis. *J Periodontal Res* 2012;47:446–454.
37. Sato T, Watanabe K, Kumada H, Toyama T, Tani-Ishii N, Hamada N. Peptidoglycan of *Actinomyces naeslundii* induces inflammatory cytokine production and stimulates osteoclastogenesis in alveolar bone resorption. *Arch Oral Biol* 2012;57:1522–1528.
38. Lahousse L, van den Bouwhuijsen QJ, Loth DW, Joos GF, Hofman A, Witteman JC, van der Lugt A, Brusselle GG, Stricker BH. Chronic obstructive pulmonary disease and lipid core carotid artery plaques in the elderly: the Rotterdam Study. *Am J Respir Crit Care Med* 2013; 187:58–64.
39. Suwa T, Hogg JC, Quinlan KB, Ohgami A, Vincent R, van Eeden SF. Particulate air pollution induces progression of atherosclerosis. *J Am Coll Cardiol* 2002;39:935–942.
40. Sin DD, Macnee W. Chronic obstructive pulmonary disease and cardiovascular diseases: a "vulnerable" relationship. *Am J Respir Crit Care Med* 2013; 187:2–4.
41. Gao Z, Dosman JA, Rennie DC, Schwartz DA, Yang IV, Beach J, Senthilselvan A. Association of Toll-like receptor 2 gene polymorphisms with lung function in workers in swine operations. *Ann Allergy Asthma Immunol* 2013;110:44–50.
42. Silhavy TJ, Kahne D, Walker S. The bacterial cell envelope. *Cold Spring Harb Perspect Biol* 2010;2:a000414.
43. Liu ZQ, Deng GM, Foster S, Tarkowski A. Staphylococcal peptidoglycans induce arthritis. *Arthritis Res* 2001;3:375–380.
44. Wang JE, Dahle MK, McDonald M, Foster SJ, Aasen AO, Thiemermann C. Peptidoglycan and lipoteichoic acid in Gram-positive bacterial sepsis: receptors, signal transduction, biological effects, and synergism. *Shock* 2003;20:402–414.